

This is the author's final, peer-reviewed manuscript as accepted for publication (AAM). The version presented here may differ from the published version, or version of record, available through the publisher's website. This version does not track changes, errata, or withdrawals on the publisher's site.

Unravelling the structural complexity of protein–lipid interactions with neutron reflectometry

Luke A Clifton

Published version information

Citation: LA Clifton. 'Unravelling the structural complexity of protein–lipid interactions with neutron reflectometry.' *Biochem Soc Trans* vol. 49, no. 4 (2021): 1537-1546.

DOI: [10.1042/BST20201071](https://doi.org/10.1042/BST20201071)

This version is made available in accordance with publisher policies. Please cite only the published version using the reference above. This is the citation assigned by the publisher at the time of issuing the AAM. Please check the publisher's website for any updates.

This item was retrieved from **ePubs**, the Open Access archive of the Science and Technology Facilities Council, UK. Please contact epublications@stfc.ac.uk or go to <http://epubs.stfc.ac.uk/> for further information and policies.

Unravelling the Structural Complexity of Protein-Lipid Interactions with Neutron Reflectometry

Luke A. Clifton

ISIS Pulsed Neutron and Muon Source, Science and Technology Facilities Council, Rutherford Appleton Laboratory, Harwell Science and Innovation Campus, Didcot, Oxfordshire, OX11 0QX, UK.

luke.clifton@stfc.ac.uk

Keywords

Biological membranes, model membranes, membrane structure, protein lipid interactions, neutron reflectometry, neutron scattering, isotopic contrast variation, protein-lipid complexes.

Abstract

Neutron reflectometry (NR) is a large-facility technique used to examine structure at interfaces. In this brief review an introduction to the utilisation of NR in the study of protein-lipid interactions is given. Cold neutron beams penetrate matter deeply, have low energies, wavelengths in the Ångstrom regime and are sensitive to light elements. High differential hydrogen sensitivity (between protium and deuterium) enables solution and sample isotopic labelling to be utilized to enhance or diminish the scattering signal of individual components within complex biological structures. The combination of these effects means NR can probe buried structures such as those at the solid liquid interface and encode molecular level structural information on interfacial protein-lipid complexes revealing the relative distribution of components as well as the overall structure. Model biological membrane sample systems can be structurally probed to examine phenomena such as antimicrobial mode of activity, as well as structural and mechanistic properties peripheral/integral proteins within membrane complexes. Here, the example of the antimicrobial protein α 1-purothionin binding to a model Gram negative bacterial outer membrane is used to highlight the utilisation of this technique, detailing how changes in the protein/lipid distributions across the membrane before and after the protein interaction can be easily encoded using hydrogen isotope labelling.

Introduction

Biological membranes are the key structural material of biology at the cellular level. Yet, due to its small transverse size and vast compositional complexity, gaining a precision understanding of membrane biochemical events can be challenging. It has long been known

31 that the diversity of membrane bound or embedded proteins was immense^[1], that this class of
32 proteins are well represented in terms of drug targets (between 40% and 60%^[2]) but under-
33 represented in the data bank of known protein structures^[3]. Perhaps the most famous group of
34 membrane proteins are the G-protein coupled receptor (GPCR) superfamily which is involved
35 in a myriad of different signalling and sensing pathways^[4], and itself, accounts for ~35% of
36 known drug targets^[5]. Other examples include the photosystem membrane complexes which
37 are key components of photosynthesis in plants and algae^[6] and the B-cell lymphoma family
38 which regulate cell death^[7].

39 Recently there has been an increased emphasis on examining the lipid components of the
40 membranes, which have been revealed to contain more complexity than once thought, with
41 over a thousand lipid types currently known across the kingdoms of life^{[8][9]}. Lipid organisation
42 within the membrane has also revealed ever increasing complexity^{[10][11]}. Many membranes
43 possess heterogeneous distributions of lipids both across and within the plane of the
44 membrane^{[4][12][13]} and there has been interest in examining the heterogeneity of lipid
45 distributions induced by membrane proteins^[13]. As most biochemical processes involve
46 membrane bound or associated proteins, the interaction of these with the lipid component of
47 the membrane are increasingly of interest in understanding membrane protein function^{[1][14][15]}.

48 Neutron reflectometry (NR) is a structural analytical tool available at large national and
49 international facilities, usually through a proposal access system. NR is unique among the
50 techniques used to resolve bio membrane structure as it is non-damaging, can probe deeply into
51 buried interfaces and, most important, resolve the relative distribution of components across
52 model biological membranes and thus can quantitatively determining the relative protein and
53 lipid distributions before and after biochemically relevant processes. In this mini-review the
54 utilisation of NR in the structural examination protein-lipid complexes is discussed. Of
55 particular interest to biochemical scientists is how this technique combined with sample and
56 solution deuterium labelling can be utilized to detail the relative distribution of macromolecular
57 components across a model biological membrane, this is therefore emphasized in the text.

58 **Neutron Scattering**

59 The use of neutron scattering as an analytical tool to examine molecular and atomic structure
60 began in earnest as a by-product of nuclear weapon and reactor development^[16]. By the late
61 1960's research reactors, such as the Institut Laue Lavengin in Grenoble, France, were being
62 built specifically to enable the use neutron scattering techniques in academic research. Neutron

63 scattering facilities fall into two categories, reactor sources in which nuclear fission provides
64 the neutron source or spallation sources in which a pulsed beam of protons are fired at a heavy
65 metal target which causes the ejection (“spallation”) of neutrons which can then be utilized in
66 scattering experiments.

67 The neutron beams used in scattering studies are generally composed of thermal, epithermal
68 and cold neutrons. These have wavelengths in the Ångstrom range, meaning the scattering of
69 these can encode Ångstrom level structural details, but have energies that are the same, slightly
70 above or below that of materials at room temperature, meaning they are essentially non-
71 damaging to biological samples. For non-magnetic samples, neutrons scatter directly from the
72 atomic nucleus. This leads to two beneficial effects, firstly neutrons can penetrate deeply into
73 matter due to the low volume the nucleus occupies. Secondly, and perhaps most importantly
74 for the biological sciences, the nuclear nature of the neutron scattering event means that the
75 neutron scattering magnitude, called the scattering length, is not coupled with atomic number
76 as is found with X-ray scattering from the electron cloud and, in fact, is random across the
77 periodic table. Elements such as carbon, nitrogen and oxygen have neutron scattering lengths
78 comparable with heavy elements such as gold, silver and lead, making neutron scattering
79 techniques sensitive to the presence of light elements.

80 Neutron scattering lengths can vary between different isotopes of same element. The scattering
81 length of the two naturally occurring forms of hydrogen, protium (~99.98% natural abundance)
82 and deuterium (~0.015% natural abundance) differ by a relatively large degree. Deuterium has
83 a scattering length similar to that of carbon while protium has a negative value. This means
84 water with natural abundance hydrogen (99.98% protium, H₂O) and heavy water (D₂O) have
85 widely different neutron scattering length densities (nSLD, scattering length divided by
86 molecular volume). The scattering length density of proteins, ribonucleic acids, lipids and
87 complex sugars, the major bio-macromolecules, are between that of H₂O and D₂O. This means
88 that by changing H₂O and D₂O mixture surrounding a bio-macromolecular complex the
89 scattering from individual components can be enhanced or diminished. By utilising this effect
90 through the collection of a series of data sets in differing H₂O and D₂O mixtures, not only can
91 the overall structure of a bio-macromolecular complex be resolved, but also, with good
92 experimental design, the relative spatial distribution of components can be encoded in the
93 scattering data. Additionally, deuterium labelling of the individual components can be used to
94 further enhance the “contrast” (difference in nSLD) between similar components and allow for

95 the distribution of domains within protein only complexes^[17] or differing lipids within a
96 membrane to be resolved^[18].

97 Differing neutron scattering techniques allow for differing questions of biological samples to
98 be answered. Macromolecular diffraction measurements allow for the understanding of
99 hydrogen distributions within high resolution protein structures^[19], quasi elastic neutron
100 scattering allows for dynamical processes within biological complexes to be probed, small
101 angle neutron scattering is a versatile molecular level probe for particle shape and distributions
102 in solution^[17] and can be utilized to examine interactions with lipid vesicles^[20]. Neutron
103 reflectometry (NR), allows for structure at interfaces to be resolved. Like small angle scattering
104 it does this with molecular precision, i.e. does not give the positions of individual atoms but
105 rather entire molecules. This technique has been used to biologically relevant interactions with
106 planar models of biological membranes^{[21][22][23][24][25][26]}.

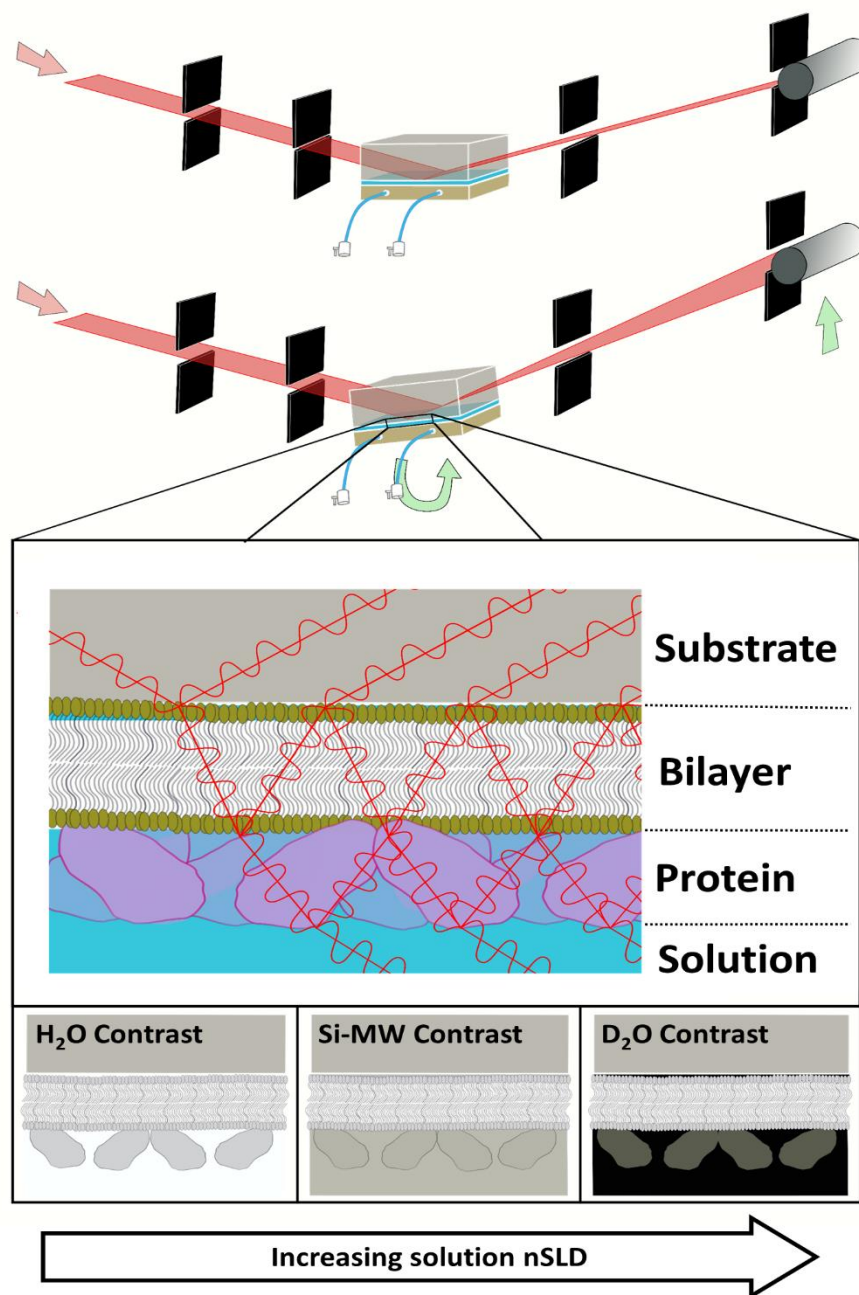
107 Dedicated NR instrumentation was first developed in the late 1980's and initially used in
108 physical/colloid chemistry and hard condensed matter physics studies^{[27][28][29][30]}. Studies on
109 lipid bilayers using NR began in the 1990's^{[31][32]}, with an increasing uptake of the technique
110 to examine model membranes^[33], membrane interactions and protein-lipid complexes since
111 this time. NR is unique in its capabilities for this science as it can readily structurally probe the
112 solid liquid interface due to the high penetration power of neutron beams. Complex biological
113 architectures such as protein-lipid complexes can be examined at the interface and the
114 compositional complexity of the structure unravelled.

115 Membrane structural and interaction studies undertaken by NR are, except in a few cases^{[34][35]},
116 on model biological membrane systems. These are planar lipid membranes, of reduced
117 complexity compared to that found *in vivo*, which allow for precise structural and biophysical
118 analysis. The complexity of the interfacial membrane models ranges from air/liquid lipid
119 monolayers which are simple yet controllable representations of a single lipid leaflet of a
120 membrane to a range of different supported lipid bilayer (SLB) types at the solid liquid
121 interface^[36]. In this mini-review I will concentrate on examining protein-lipid interactions with
122 supported lipid bilayers. In its simplest form these model membrane constructs are composed
123 of lipid bilayers deposited onto a solid substrate material by Langmuir Blodgett/ Langmuir
124 Schaefer deposition^[37] or vesicle rupture^[38]. More biologically accurate advanced models
125 include polymer cushioned, surface tethered and floating planar membrane systems^{[39][40][41]}.
126 The examination of lipid nanodiscs with and without embedded proteins at interfaces has been

127 an area of interest for reflectometry studies in recent years [42][43][44][45], with peptide coated
128 nanodiscs being used recently to create supported lipid bilayers containing well orientated
129 integral membrane proteins[46].

130 NR examination of model membrane sample systems can complement studies using atomic
131 force microscopy[47], solid state NMR spectroscopy[48], quartz crystal microbalance
132 measurements[49], Cryo-electron microscopy[50], surface plasmon resonance[51] and
133 ellipsometry[52] with NR, uniquely, providing the complex structure across the membrane.

134



135

136 **Figure 1, a schematic representation of a neutron reflectometry beamline, the process of reflection and**
137 **refraction through a protein bound SLB at the solid/liquid interface and the use of solution isotopic contrast**
138 **to sensitize the experimental reflectivity profiles to differing components of this interfacial protein-lipid**
139 **complex.** A collimated beam of neutrons illuminates the solid/liquid interface within a flow cell, the angle of the
140 sample surface and the detector relative to the incoming neutron beam are increased to probe higher Q_z values
141 (A). At the solid liquid interface reflection and refraction will occur at the interfaces of any layered material
142 present giving rise to an interference pattern in the NR data in the form of Kiessig fringes, a protein bound SLB
143 is shown as an example of such an interfacial structure (B). Changing the ratio of H_2O and D_2O within the sample
144 cell can enhance or reduce the contribution of differing components of the protein-lipid complex to the
145 reflectometry data (C).

146 Neutrons are reflected and refracted at interfacial scattering length density boundaries such as
147 the solid/liquid, air/liquid or solid/air interfaces (Fig 1, B). The relative magnitude of reflection
148 vs. refraction is related on the angle of incidence, neutron wavelength and difference in nSLD
149 between the bulk phases (as described by Fresnel for the reflection of light^[53]). In NR the
150 reflected intensity is measured against Q_z (wave vector transfer in the Z direction i.e. normal
151 to the interface or out-of-plane) which is a convenient way to combine data collected at
152 different angles and wavelengths with:

$$153 \quad Q_z = \frac{4\pi \sin\theta}{\lambda}$$

154 Therefore Q_z is proportional to the incident angle (θ) and inversely proportional to the
155 wavelength (λ). For a bare interface the reflectivity intensity will decay with a gradient
156 proportional to Q_z^{-4} . If any material is present at the interface (such as the protein bound SLB
157 shown in Fig 1B), and has a difference in scattering length density (also referred to as contrast)
158 from its surrounding environment, reflections will occur on both the upper and lower sides of
159 this material (we describe this as a layer). The interference between these reflections will give
160 rise to oscillations in the NR data known as Kiessig fringes^[3]. The repeat distance of the fringes
161 in Q_z is inversely proportional to thickness of the layer while the amplitude of the constructive
162 regions is proportional to the difference in nSLD between the layer and its surroundings, which
163 is connected to the identity of the material through knowledge of its chemical composition and
164 isotopic labelling. If the surrounding media is water, changing the H_2O and D_2O ratio will
165 modify the intensity of these fringes, highlighting or dampening the contribution from an
166 individual layer/component to the NR data. In these studies, heavy water (D_2O) and water
167 (H_2O) buffers are produced using the same methodology with the exception that the measured
168 pH probe reading of the D_2O solution should be 0.45 lower than that of the water (H_2O) buffer

169 solution to account for the weaker acidity of deuterons compared to protons and produce a pD
170 value which matches the pH of the H₂O buffer solution^[54].

171 Reflectometry data from biological macromolecular complexes is often a superposition of
172 Kiessig fringes produced by multiple individual components. Figure 1. C shows a series of
173 schematic contrast diagrams from a protein-lipid complex. Here shading is used to represent
174 nSLD, the darker the shade the higher the nSLD value. By changing the nSLD of the solution
175 through D₂O/H₂O exchange, the contribution of differing components of a protein-lipid
176 complex (in Fig 1 C, a protein bound supported lipid bilayer) can be highlighted or reduced in
177 the reflectivity data. Lipid tails, for example, have an nSLD similar to that of H₂O, meaning
178 this solution contrast will be more sensitive to the structural distribution of the head groups and
179 the protein component (and less sensitive to the tail structure). Conversely, in silicon matched
180 water (Si-MW, 38% D₂O) the nSLD of the lipid head groups and protein component will be
181 close to the solution (i.e. “matched out”), meaning this contrast will be mainly sensitive to the
182 lipid tail distribution. All components, lipid tails, head groups and protein will contribute to the
183 NR data in D₂O meaning this contrast describes the overall envelope of the protein-lipid
184 complex. By combined fitting of all three data sets not only is the overall structure of the
185 complex best resolved but the relative distribution of components within that complex is
186 unambiguously elucidated. For a quantitative description on the use solution contrast in NR
187 studies on protein-lipid complexes see a recent article by Heinrich *et al* ^[55].

188 As well a solution isotope labelling, deuterium labelling of components within the membrane
189 complex allows for additional manipulation of nSLD and is particularly useful when there is a
190 need to resolve the relative distributions of two similar components (or components of similar
191 nSLD), such as determining the organisation of different lipid types across the membrane^{[18][56]}.
192 Figure 2 shows an example of this for the interaction of the antimicrobial seed defence protein
193 α 1-purothionin (-Pth) with a supported lipid bilayer model of the Gram negative bacterial outer
194 membrane. This type of model membrane system was the topic of a recent review by us^[57] and
195 is composed of a biologically relevant asymmetric distribution of phospholipid and rough
196 mutant bacterial lipopolysaccharides on a silicon support surface^[18]. The relative distribution
197 of components across the model membrane both before and after the interaction of α 1-Pth is
198 resolved from simultaneously fitting the three isotopic contrasts (Fig 2, A, 100% D₂O, Si-MW
199 (38% D₂O) and 100% H₂O).

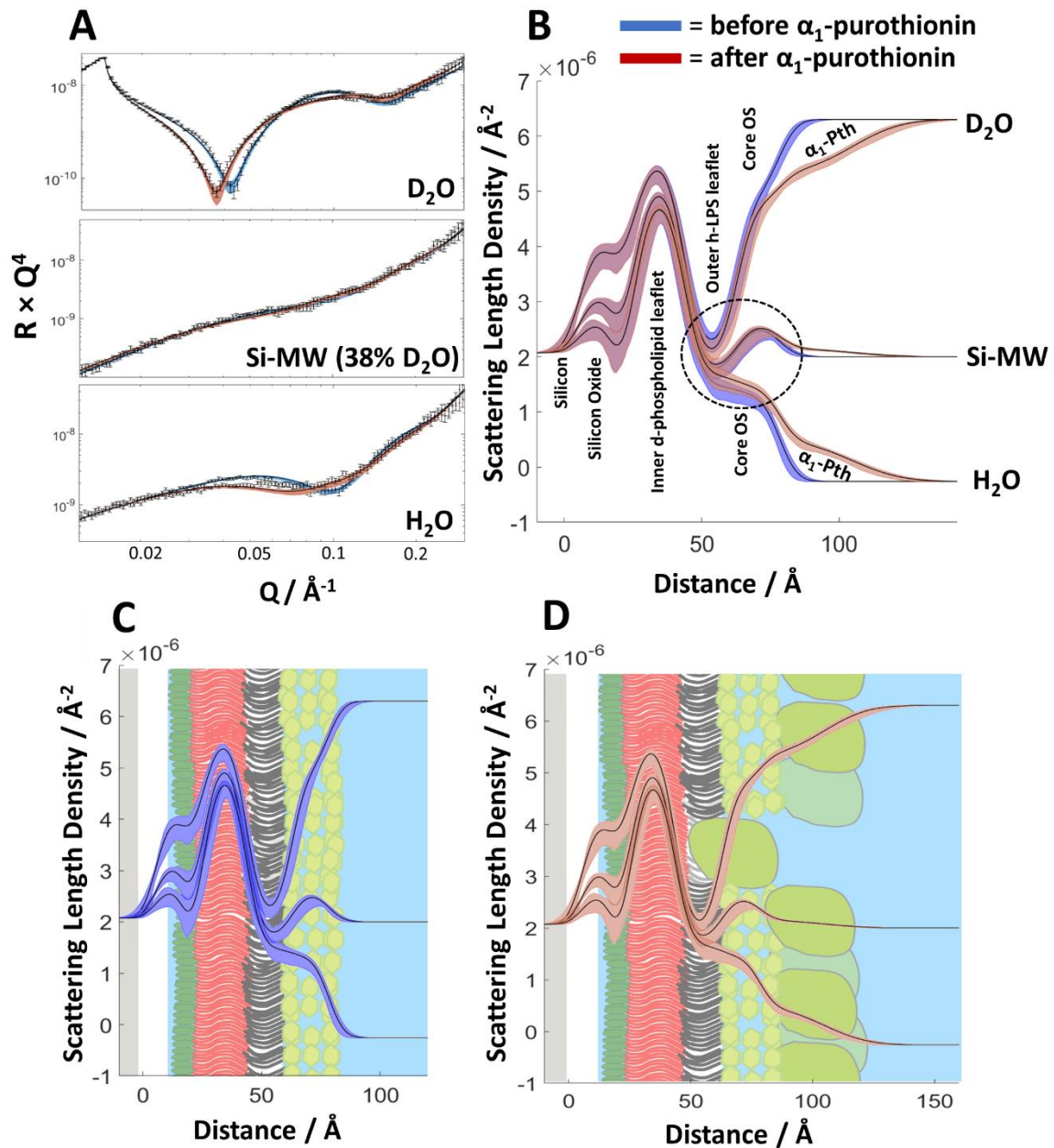
200 Deuterium labelling of the phospholipid component (inner leaflet) allows the relative
201 distribution of this and the hydrogenous (natural abundance hydrogen) lipopolysaccharide to
202 be resolved across the SLB. The deuterated phospholipid tails dominate the reflectivity in the
203 H₂O contrast data sets, while the h-LPS tails are prevalent in the D₂O data sets. Both
204 components contribute to the Si-MW data set. The position of the core oligosaccharide is well
205 defined in both the D₂O and H₂O data sets due to the intermediate nSLD values of this
206 component ($\sim 2 \times 10^{-6} \text{ \AA}^{-2}$ in H₂O and $\sim 4 \times 10^{-6} \text{ \AA}^{-2}$ in D₂O^[18], the difference between the two
207 being due to the exchange of labile hydrogens with their surroundings). The analysis of the NR
208 produces nSLD vs. distance profiles (shown in Fig 2 B, C and D, note that distance is on the Å
209 scale). The data prior to the α1-Pth binding is shown in blue (Fig 2 B) while the data after
210 protein binding is shown in red (Fig 2 C). Like the core oligosaccharide the protein component
211 of the membrane has an intermediate nSLD (between that of H₂O and D₂O) being $1.9 \times 10^{-6} \text{ \AA}^{-2}$
212 in H₂O and $3.2 \times 10^{-6} \text{ \AA}^{-2}$ in D₂O, meaning the protein distribution across the membrane is
213 encoded for in both the D₂O and H₂O contrasts. Conversely, the Si-MW solution is near the
214 match point of the protein ($\sim 42\%$ D₂O) so will not contain significant information about this
215 component.

216 From the nSLD profile prior to α1-Pth binding (Fig 2 B) we identify a sinusoidal shape across
217 the membrane moving away from the bulk interface ($> 0 \text{ \AA}$ on the plot, Fig. 2 B and C), due to
218 the high nSLD of the inner leaflet phospholipid tails and the low nSLD of the outer leaflet h-
219 LPS tails. Next to this (again moving away from the bulk interface) is the core oligosaccharide
220 region of the LPS on the outer surface of the bilayer. This layer is highly hydrated hence the
221 strong difference in nSLD between this region in the nSLD profiles of the D₂O and H₂O data
222 sets (Fig 2 C). Adjacent to the core oligosaccharide is the bulk solution.

223 Upon the interaction of α1-Pth with the model membrane the lipid distribution remains
224 unchanged, but we can observe the presence of a new, diffuse and highly hydrated layer of
225 protein on the surface of the membrane (Fig 2 B and D). The thickness of this layer was found
226 to be $\sim 26 \text{ \AA}$ and the membrane surface coverage of protein (not including protein hydrating
227 water) was $\sim 35\%$. A comparison of this thickness with the crystal structure suggest a single
228 layer of bound thionin to the outer surface of the membrane^[58]. The comparison of the nSLD
229 of the outer (LPS) tails before and after protein interaction suggests that a small proportion of
230 the bound protein ($\leq 10\%$ volume fraction) had penetrated into the LPS tail and the core
231 oligosaccharide region of the outer membrane outer leaflet. This can be seen in fig 2B where
232 there is a difference in the nSLD of the tail and core regions upon protein binding Fig 2 B

233 dotted circle). Although this change was not determined to be significant by ambiguity analysis
234 (ambiguity of the resolved structure is shown as a line width). A conclusive assessment of the
235 membrane penetration by NR would come through repeating this experiment using a differing
236 isotopic contrast series. An optimised contrast strategy for this interaction would be to examine
237 a deuterated form the protein interacting with a fully hydrogenous SLB, as larger changes in
238 the experimental reflectometry profiles in H₂O/Si-MW would be observed from the protein
239 density distribution across the membrane yielding a less ambiguous identification of protein
240 penetration into the membrane (Fig 3 shows a contrast diagrams comparing these two differing
241 labelling strategies).

242



243

244

245 **Figure 2, Neutron reflectometry data and associated scattering length density profiles for a model Gram**
 246 **negative outer membrane prior to and after the interaction of the antimicrobial protein $\alpha 1$ -purothionin.**

247 The NR data was collected under three solution isotopic contrast conditions, before and after protein binding,
 248 deuterium labelling of inner membrane leaflet phospholipid was used to differentiate this from the
 249 lipopolysaccharide (A). NR data is shown in an $R \times Q^4$ format to remove the inherent Q^{-4} gradient on the data and
 250 highlight the Keissig fringes. Combining the bilayer and solution hydrogen isotope labelling approaches allowed
 251 for the relative distribution of the phospholipid, lipopolysaccharide, water and protein across the membrane to be
 252 determined through interrogation of the scattering length density profiles (B, C and D). The nSLD profiles overlaid
 253 onto a schematic representation of the surface structure before (C) and after (D) the interaction $\alpha 1$ -Pth are given.

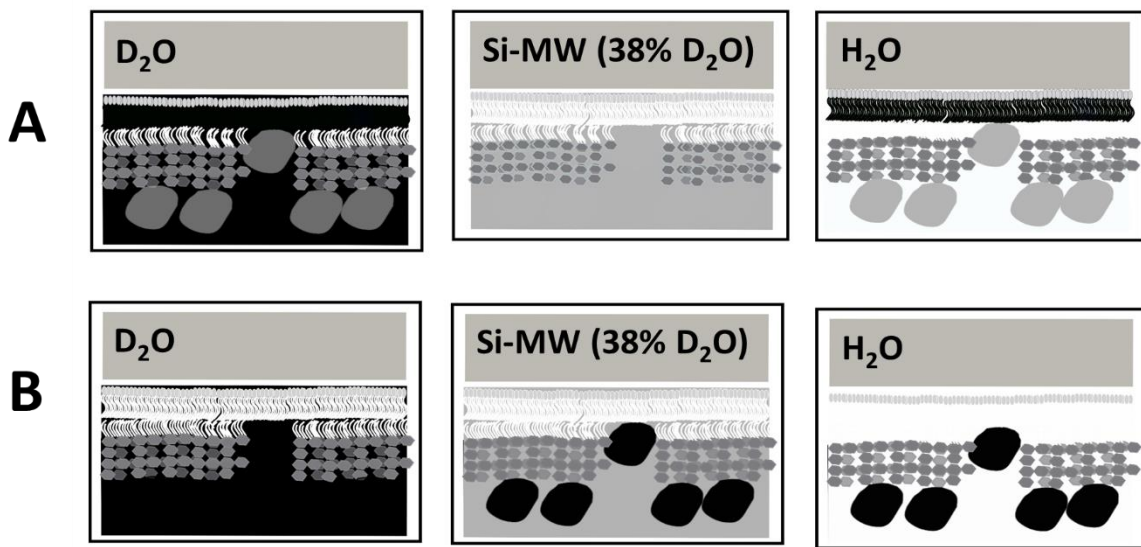
254 It should be noted the membrane bound protein distribution was conclusively resolved while the membrane
255 penetrated protein distribution was not.

256 **NR Studies on protein-lipid complexes**

257 Figure 2 shows antimicrobial protein disruption of a model membrane by a lipid interacting
258 antimicrobial compounds. This area of study is increasingly utilising NR's ability to provide
259 structural insights into the mechanisms of antimicrobial activity by elucidating the resulting
260 changes in the distribution of components across the membrane (like the example shown).
261 Examples of this are in studies on peptide disruption of lipid monolayers^[23] and venom toxin
262 disruption of supported lipid bilayers^[22]. Recently NR has been used to examine the
263 antimicrobial activity of new peptide based antibiotics^{[25][59][60][61]} and provide a precision
264 understanding of the activity of natural antimicrobial peptides^{[21][62][63][64]}. Biochemically
265 relevant protein-lipid interactions are another area where NR is able to provide unique insights.
266 Information such as the protein distribution relative to the membrane surface^[65] and the
267 orientation of surface bound peripheral membrane proteins^[66] provides unique molecular level
268 insights into membrane biochemistry. Integral membrane protein distribution within the lipid
269 matrix is an increasingly utilized area. Currently this has been used to benchmark
270 biotechnological sensor systems^[67] or new integral membrane protein containing membrane
271 sample systems^{[68][46]}. Biochemical structural studies on integral membrane proteins provide a
272 means of structurally probing function within the membrane environment^{[48][69][70][71]}.

273 For further reading about examples of the biological work undertaken with NR please refer to
274 review articles by Gerelli^[72], Wacklin^[73], Lakey^[74], Heinrich and Lösche^[75] and Fragneto *et*
275 *al*^[76]. More technical details on performing NR experiments to examine protein-lipid
276 interactions can be found in a methods chapter by us^[77]. Additionally, we recently published a
277 techniques review article detailing how to use a series of complementary analytical techniques,
278 including NR, to examine interactions with planar membrane models^[36] and an article detailing
279 the application of a variety of neutron scattering techniques to study biological membranes^[20].

280



281

282 **Figure 3, Contrast diagram comparing the two differing isotopic labelling strategies used to examine the**
 283 **distribution of components across a model biological membrane.** The contrast diagram of the labelling strategy
 284 used in figure 2 is shown (A), this gives a good structural description of the lipid distribution and is sensitive to
 285 the protein distribution but less so than deuterated protein interacting with a fully hydrogenous SLB (B), however,
 286 in the latter case we would lose sensitivity to the lipid distribution as a result.

287 **Outlook**

288 The applied use of neutron reflectometry for unravelling the structural complexity of protein-
 289 lipid interactions is still in its infancy. However, examples of the utilisation of this technique
 290 are growing and biologists using NR beamlines to answer questions of membrane biology is
 291 becoming more commonplace. New instrumentation is being built with this science as one of
 292 the major drivers and most facilities now employ scientists who specialize in developing and
 293 assisting users with bio related NR studies, enabling more complex and sophisticated structural
 294 studies to be undertaken. Key to the continued advance of this technique is a drive towards
 295 accurate *in vitro* membrane models that allow for precision structural data to be obtained under
 296 biologically accurate conditions and advances in data analysis, particularly towards the
 297 incorporation of molecular dynamics simulations.

298 **Accessing NR instrumentation**

299 Biologists interested in undertaking NR studies should contact their nearest neutron scattering
 300 facility who will put them in contact with facility scientists who will guide the novice on the
 301 mechanisms by which experimental beam time can be sought and provide the expertise and
 302 sample environment required to enable experimental success.

303 **Perspectives**

- 304 • Neutron reflectometry is a powerful technique that is uniquely able to structurally
305 resolve the compositional complexity within model biological membranes.
- 306 • Key to the utilisation of this technique is the use of solution and sample deuterium
307 labelling and accurate model membrane systems.
- 308 • Future improvements in model membrane systems, data collection times and analysis
309 strategies will allow for ever increasing and complex membrane relevant biochemical
310 interactions to be examined using NR.

311 **Acknowledgements**

312 I would like to thank Professor Jeremy Lakey, Dr John Webster, Dr Maximillian Skoda and Dr
313 Stephen Hall for helpful advice and support when writing this review article. This article was
314 supported by ISIS Pulsed Neutron and Muon Source for beam time award (RB1310101). No
315 additional funding sources are associated with the review.

316 I declare no conflict of interest.

317 **Bibliography**

- 318 [1] Corradi V, Sejdiu BI, Mesa-Galloso H, Abdizadeh H, Noskov SY, Marrink SJ, et al.
319 (2019) Emerging Diversity in Lipid-Protein Interactions. *Chem. Rev.* **119**, 5775–5848.
- 320 [2] Arinaminpathy Y, Khurana E, Engelman DM, Gerstein MB. (2009) Computational
321 analysis of membrane proteins: the largest class of drug targets. *Drug Discov. Today*
322 [Internet]. **14**, 1130–1135. Available from:
323 <https://linkinghub.elsevier.com/retrieve/pii/S1359644609002827>
- 324 [3] Hendrickson WA. (2016) Atomic-level analysis of membrane-protein structure. *Nat.*
325 *Struct. Mol. Biol.* [Internet]. **23**, 464–467. Available from:
326 <http://www.nature.com/articles/nsmb.3215>
- 327 [4] Katritch V, Cherezov V, Stevens RC. (2013) Structure-Function of the G Protein–
328 Coupled Receptor Superfamily. *Annu. Rev. Pharmacol. Toxicol.* [Internet]. **53**, 531–
329 556. Available from: [http://www.annualreviews.org/doi/10.1146/annurev-pharmtox-](http://www.annualreviews.org/doi/10.1146/annurev-pharmtox-032112-135923)
330 [032112-135923](http://www.annualreviews.org/doi/10.1146/annurev-pharmtox-032112-135923)
- 331 [5] Hauser AS, Attwood MM, Rask-Andersen M, Schiöth HB, Gloriam DE. (2017)
332 Trends in GPCR drug discovery: new agents, targets and indications. *Nat. Rev. Drug*

- 333 Discov. [Internet]. **16**, 829–842. Available from:
334 <http://www.nature.com/articles/nrd.2017.178>
- 335 [6] Mazor Y, Borovikova A, Nelson N. (2015) The structure of plant photosystem I super-
336 complex at 2.8 Å resolution. *Elife* [Internet]. **4**. Available from:
337 <https://elifesciences.org/articles/07433>
- 338 [7] Tatulian SA. (2003) Attenuated Total Reflection Fourier Transform Infrared
339 Spectroscopy: A Method of Choice for Studying Membrane Proteins and Lipids † .
340 *Biochemistry*. **42**, 11898–11907.
- 341 [8] Kuo TC, Tseng YJ. (2018) LipidPedia: A comprehensive lipid knowledgebase.
342 *Bioinformatics*. **34**, 2982–2987.
- 343 [9] Fahy E, Subramaniam S, Brown HA, Glass CK, Merrill AH, Murphy RC, et al. (2005)
344 A comprehensive classification system for lipids. *J. Lipid Res*. **46**, 839–861.
- 345 [10] Harayama T, Riezman H. (2018) Understanding the diversity of membrane lipid
346 composition. *Nat. Rev. Mol. Cell Biol.* [Internet]. **19**, 281–296. Available from:
347 <http://dx.doi.org/10.1038/nrm.2017.138>
- 348 [11] Muro E, Atilla-Gokcumen GE, Eggert US. (2014) Lipids in cell biology: how can we
349 understand them better? *Mol. Biol. Cell* [Internet]. **25**, 1819–1823. Available from:
350 <https://www.molbiolcell.org/doi/10.1091/mbc.e13-09-0516>
- 351 [12] Ingólfsson HI, Melo MN, van Eerden FJ, Arnarez C, Lopez CA, Wassenaar TA, et al.
352 (2014) Lipid Organization of the Plasma Membrane. *J. Am. Chem. Soc.* [Internet].
353 **136**, 14554–14559. Available from: <https://pubs.acs.org/doi/10.1021/ja507832e>
- 354 [13] Carquin M, D’Auria L, Pollet H, Bongarzone ER, Tyteca D. (2016) Recent progress
355 on lipid lateral heterogeneity in plasma membranes: From rafts to submicrometric
356 domains. *Prog. Lipid Res.* [Internet]. **62**, 1–24. Available from:
357 <https://linkinghub.elsevier.com/retrieve/pii/S016378271530014X>
- 358 [14] Escribá P V., Wedegaertner PB, Goñi FM, Vögler O. (2007) Lipid-protein interactions
359 in GPCR-associated signaling. *Biochim. Biophys. Acta - Biomembr.* **1768**, 836–852.
- 360 [15] Laganowsky A, Reading E, Allison TM, Ulmschneider MB, Degiacomi MT, Baldwin
361 AJ, et al. (2014) Membrane proteins bind lipids selectively to modulate their structure
362 and function. *Nature* [Internet]. **510**, 172–175. Available from:

- 363 <http://www.nature.com/articles/nature13419>
- 364 [16] Mason TE, Gawne TJ, Nagler SE, Nestor MB, Carpenter JM. (2013) The early
365 development of neutron diffraction: science in the wings of the Manhattan Project.
366 *Acta Crystallogr. Sect. A Found. Crystallogr.* [Internet]. **69**, 37–44. Available from:
367 <http://scripts.iucr.org/cgi-bin/paper?S0108767312036021>
- 368 [17] Neylon C. (2008) Small angle neutron and X-ray scattering in structural biology:
369 recent examples from the literature. *Eur. Biophys. J.* , 28–30.
- 370 [18] Clifton LA, Skoda MWA, Daulton EL, Hughes A V, Le Brun AP, Lakey JH, et al.
371 (2013) Asymmetric phospholipid: lipopolysaccharide bilayers; a Gram-negative
372 bacterial outer membrane mimic. *J. R. Soc. Interface* [Internet]. **10**, 20130810.
373 Available from: <https://royalsocietypublishing.org/doi/10.1098/rsif.2013.0810>
- 374 [19] O’Dell WB, Bodenheimer AM, Meilleur F. (2016) Neutron protein crystallography: A
375 complementary tool for locating hydrogens in proteins. *Arch. Biochem. Biophys.*
376 [Internet]. **602**, 48–60. Available from:
377 <https://linkinghub.elsevier.com/retrieve/pii/S0003986115301041>
- 378 [20] Qian S, Sharma VK, Clifton LA. (2020) Understanding the Structure and Dynamics of
379 Complex Biomembrane Interactions by Neutron Scattering Techniques. *Langmuir*
380 [Internet]. **36**, 15189–15211. Available from:
381 <https://pubs.acs.org/doi/10.1021/acs.langmuir.0c02516>
- 382 [21] Wang CK, Wacklin HP, Craik DJ. (2012) Cyclotides insert into lipid bilayers to form
383 membrane pores and destabilize the membrane through hydrophobic and
384 phosphoethanolamine-specific interactions. *J. Biol. Chem.* **287**, 43884–43898.
- 385 [22] Vacklin HP, Tiberg F, Fragneto G, Thomas RK. (2005) Phospholipase A2 hydrolysis
386 of supported phospholipid bilayers: a neutron reflectivity and ellipsometry study.
387 *Biochemistry* [Internet]. **44**, 2811–21. Available from:
388 <http://www.ncbi.nlm.nih.gov/pubmed/15723525>
- 389 [23] Lad MD, Birembaut F, Clifton LA, Frazier RA, Webster JRP, Green RJ. (2007)
390 Antimicrobial peptide-lipid binding interactions and binding selectivity. *Biophys. J.*
391 **92**, 3575–3586.
- 392 [24] Clifton LA, Ciesielski F, Skoda MWA, Paracini N, Holt SA, Lakey JH. (2016) The

- 393 Effect of Lipopolysaccharide Core Oligosaccharide Size on the Electrostatic Binding
394 of Antimicrobial Proteins to Models of the Gram Negative Bacterial Outer Membrane.
395 *Langmuir* [Internet]. , acs.langmuir.6b00240. Available from:
396 <http://pubs.acs.org/doi/abs/10.1021/acs.langmuir.6b00240>
- 397 [25] Gong H, Sani MA, Hu X, Fa K, Hart JW, Liao M, et al. (2020) How do Self-
398 Assembling Antimicrobial Lipopeptides Kill Bacteria? *ACS Appl. Mater. Interfaces*.
- 399 [26] Barros M, Heinrich F, Datta SAK, Rein A, Karageorgos I, Nanda H, et al. (2016)
400 Membrane Binding of HIV-1 Matrix Protein: Dependence on Bilayer Composition and
401 Protein Lipidation. *J. Virol.* [Internet]. **90**, 4544–4555. Available from:
402 <http://jvi.asm.org/lookup/doi/10.1128/JVI.02820-15>
- 403 [27] Penfold J, Thomas RK. (1990) The application of the specular reflection of neutrons to
404 the study of surfaces and interfaces. *J. Phys. Condens. Matter* [Internet]. **2**, 1369–1412.
405 Available from: <https://iopscience.iop.org/article/10.1088/0953-8984/2/6/001>
- 406 [28] Lu JR, Li ZX, Thomas RK, Staples EJ, Tucker I, Penfold J. (1993) Neutron reflection
407 from a layer of monododecyl hexaethylene glycol adsorbed at the air-liquid interface:
408 the configuration of the ethylene glycol chain. *J. Phys. Chem.* [Internet]. **97**, 8012–
409 8020. Available from: <https://pubs.acs.org/doi/abs/10.1021/j100132a034>
- 410 [29] Penfold J, Ward RC, Williams WG. (1987) A time-of-flight neutron reflectometer for
411 surface and interfacial studies. *J. Phys. E.* [Internet]. **20**, 1411–1417. Available from:
412 <https://iopscience.iop.org/article/10.1088/0022-3735/20/11/024>
- 413 [30] Penfold J, Richardson RM, Zarbakhsh A, Webster JRP, Bucknall DG, Rennie AR, et
414 al. (1997) Recent advances in the study of chemical surfaces and interfaces by specular
415 neutron reflection. *J. Chem. Soc. Faraday Trans.* [Internet]. **93**, 3899–3917. Available
416 from: <http://xlink.rsc.org/?DOI=a702836i>
- 417 [31] Johnson SJ, Bayerl TM, McDermott DC, Adam GW, Rennie AR, Thomas RK, et al.
418 (1991) Structure of an adsorbed dimyristoylphosphatidylcholine bilayer measured with
419 specular reflection of neutrons. *Biophys. J.* [Internet]. **59**, 289–294. Available from:
420 <https://linkinghub.elsevier.com/retrieve/pii/S0006349591822226>
- 421 [32] Koenig BW, Krueger S, Orts WJ, Majkrzak CF, Berk NF, Silverton J V., et al. (1996)
422 Neutron Reflectivity and Atomic Force Microscopy Studies of a Lipid Bilayer in

- 423 Water Adsorbed to the Surface of a Silicon Single Crystal. *Langmuir* [Internet]. **12**,
424 1343–1350. Available from: <https://pubs.acs.org/doi/10.1021/la950580r>
- 425 [33] Fragneto G, Charitat T, Graner F, Mecke K, Perino-Gallice L, Bellet-Amalric E.
426 (2001) A fluid floating bilayer. *Europhys. Lett.* [Internet]. **53**, 100–106. Available
427 from: <https://iopscience.iop.org/article/10.1209/epl/i2001-00129-8>
- 428 [34] Smith HL, Hickey J, Jablin MS, Trujillo A, Freyer JP, Majewski J. (2010) Mouse
429 Fibroblast Cell Adhesion Studied by Neutron Reflectometry. *Biophys. J.* [Internet]. **98**,
430 793–799. Available from:
431 <https://linkinghub.elsevier.com/retrieve/pii/S0006349509017470>
- 432 [35] Junghans A, Waltman MJ, Smith HL, Pocivavsek L, Zebda N, Birukov K, et al. (2014)
433 Understanding dynamic changes in live cell adhesion with neutron reflectometry. *Mod.*
434 *Phys. Lett. B* [Internet]. **28**, 1430015. Available from:
435 <https://www.worldscientific.com/doi/abs/10.1142/S0217984914300154>
- 436 [36] Clifton LA, Campbell RA, Sebastiani F, Campos-Terán J, Gonzalez-Martinez JF,
437 Björklund S, et al. (2020) Design and use of model membranes to study biomolecular
438 interactions using complementary surface-sensitive techniques. *Adv. Colloid Interface*
439 *Sci.* [Internet]. **277**, 102118. Available from:
440 <https://linkinghub.elsevier.com/retrieve/pii/S0001868619304440>
- 441 [37] Kurniawan J, Ventrici De Souza JF, Dang AT, Liu GY, Kuhl TL. (2018) Preparation
442 and Characterization of Solid-Supported Lipid Bilayers Formed by Langmuir-Blodgett
443 Deposition: A Tutorial. *Langmuir*. **34**, 15622–15639.
- 444 [38] Richter RP, Bérat R, Brisson AR. (2006) Formation of solid-supported lipid bilayers:
445 An integrated view. *Langmuir*. **22**, 3497–3505.
- 446 [39] Sackmann E. (1996) Supported membranes: scientific and practical applications.
447 *Science* [Internet]. **271**, 43–8. Available from:
448 <http://www.ncbi.nlm.nih.gov/pubmed/8539599>
- 449 [40] Tanaka M, Sackmann E. (2005) Polymer-supported membranes as models of the cell
450 surface. *Nature*. **437**, 656–663.
- 451 [41] Smith HL, Jablin MS, Vidyasagar A, Saiz J, Watkins E, Toomey R, et al. (2009)
452 Model Lipid Membranes on a Tunable Polymer Cushion. *Phys. Rev. Lett.* [Internet].

- 453 **102**, 228102. Available from:
454 <https://link.aps.org/doi/10.1103/PhysRevLett.102.228102>
- 455 [42] Hall SCL, Clifton LA, Tognoloni C, Morrison KA, Knowles TJ, Kinane CJ, et al.
456 (2020) Adsorption of a styrene maleic acid (SMA) copolymer-stabilized phospholipid
457 nanodisc on a solid-supported planar lipid bilayer. *J. Colloid Interface Sci.* [Internet].
458 **574**, 272–284. Available from:
459 <https://linkinghub.elsevier.com/retrieve/pii/S0021979720304525>
- 460 [43] Wadsäter M, Laursen T, Singha A, Hatzakis NS, Stamou D, Barker R, et al. (2012)
461 Monitoring Shifts in the Conformation Equilibrium of the Membrane Protein
462 Cytochrome P450 Reductase (POR) in Nanodiscs*. *J. Biol. Chem.* [Internet]. **287**,
463 34596–34603. Available from:
464 <https://linkinghub.elsevier.com/retrieve/pii/S0021925820627922>
- 465 [44] Bertram N, Laursen T, Barker R, Bavishi K, Møller BL, Cárdenas M. (2015) Nanodisc
466 Films for Membrane Protein Studies by Neutron Reflection: Effect of the Protein
467 Scaffold Choice. *Langmuir* [Internet]. **31**, 8386–8391. Available from:
468 <https://pubs.acs.org/doi/10.1021/acs.langmuir.5b00936>
- 469 [45] Hazell G, Arnold T, Barker RD, Clifton LA, Steinke N-J, Tognoloni C, et al. (2016)
470 Evidence of Lipid Exchange in Styrene Maleic Acid Lipid Particle (SMALP)
471 Nanodisc Systems. *Langmuir*. **32**.
- 472 [46] Luchini A, Tidemand FG, Johansen NT, Campana M, Sotres J, Ploug M, et al. (2020)
473 Peptide Disc Mediated Control of Membrane Protein Orientation in Supported Lipid
474 Bilayers for Surface-Sensitive Investigations. *Anal. Chem.* [Internet]. **92**, 1081–1088.
475 Available from: <https://pubs.acs.org/doi/10.1021/acs.analchem.9b04125>
- 476 [47] Mingeot-Leclercq M-P, Deleu M, Brasseur R, Dufrêne YF. (2008) Atomic force
477 microscopy of supported lipid bilayers. *Nat. Protoc.* [Internet]. **3**, 1654–1659.
478 Available from: <http://www.nature.com/articles/nprot.2008.149>
- 479 [48] Mushtaq AU, Ådén J, Clifton LA, Wacklin-Knecht H, Campana M, Dingeldein APG,
480 et al. (2021) Neutron reflectometry and NMR spectroscopy of full-length Bcl-2 protein
481 reveal its membrane localization and conformation. *Commun. Biol.* [Internet]. **4**, 507.
482 Available from: <http://www.nature.com/articles/s42003-021-02032-1>

- 483 [49] Keller CA, Glasmästar K, Zhdanov VP, Kasemo B. (2000) Formation of Supported
484 Membranes from Vesicles. *Phys. Rev. Lett.* **84**, 5443–5446.
- 485 [50] Yao X, Fan X, Yan N. (2020) Cryo-EM analysis of a membrane protein embedded in
486 the liposome. *Proc. Natl. Acad. Sci.* [Internet]. **117**, 18497–18503. Available from:
487 <http://www.pnas.org/lookup/doi/10.1073/pnas.2009385117>
- 488 [51] Parkkila P, Elderdfi M, Bunker A, Viitala T. (2018) Biophysical Characterization of
489 Supported Lipid Bilayers Using Parallel Dual-Wavelength Surface Plasmon
490 Resonance and Quartz Crystal Microbalance Measurements. *Langmuir* [Internet]. **34**,
491 8081–8091. Available from: <https://pubs.acs.org/doi/10.1021/acs.langmuir.8b01259>
- 492 [52] Kamble S, Patil S, Kulkarni M, Murthy AVR. (2019) Spectroscopic Ellipsometry of
493 fluid and gel phase lipid bilayers in hydrated conditions. *Colloids Surfaces B*
494 *Biointerfaces* [Internet]. **176**, 55–61. Available from:
495 <https://linkinghub.elsevier.com/retrieve/pii/S0927776518309421>
- 496 [53] Born M, Wolf E. (1999) *Principles of Optics* [Internet]. Cambridge University Press;
497 1999. Available from:
498 <https://www.cambridge.org/core/product/identifier/9781139644181/type/book>
- 499 [54] Krężel A, Bal W. (2004) A formula for correlating p K a values determined in D 2 O
500 and H 2 O. *J. Inorg. Biochem.* [Internet]. **98**, 161–166. Available from:
501 <https://linkinghub.elsevier.com/retrieve/pii/S0162013403004008>
- 502 [55] Heinrich F, Kienzle PA, Hoogerheide DP, Lösche M. (2020) Information gain from
503 isotopic contrast variation in neutron reflectometry on protein–membrane complex
504 structures. *J. Appl. Crystallogr.* [Internet]. **53**, 800–810. Available from:
505 <http://scripts.iucr.org/cgi-bin/paper?S1600576720005634>
- 506 [56] Wacklin HP. (2011) Composition and Asymmetry in Supported Membranes Formed
507 by Vesicle Fusion. *Langmuir* [Internet]. **27**, 7698–7707. Available from:
508 <https://pubs.acs.org/doi/10.1021/la200683e>
- 509 [57] Paracini N, Clifton LA, Lakey JH. (2020) Studying the surfaces of bacteria using
510 neutron scattering: finding new openings for antibiotics. *Biochem. Soc. Trans.*
511 [Internet]. **48**, 2139–2149. Available from:
512 <https://portlandpress.com/biochemsoctrans/article/48/5/2139/226559/Studying-the->

- 513 surfaces-of-bacteria-using-neutron
- 514 [58] Rao U, Stec B, Teeter MM. (1995) Refinement of purothionins reveals solute particles
515 important for lattice formation and toxicity. Part 1: alpha1-purothionin revisited. *Acta*
516 *Crystallogr D Biol Crystallogr.* **51**, 904–913.
- 517 [59] Gong H, Liao M, Hu X, Fa K, Phanphak S, Ciumac D, et al. (2020) Aggregated
518 Amphiphilic Antimicrobial Peptides Embedded in Bacterial Membranes. *ACS Appl.*
519 *Mater. Interfaces* [Internet]. **12**, 44420–44432. Available from:
520 <https://pubs.acs.org/doi/10.1021/acsami.0c09931>
- 521 [60] Ciumac D, Campbell RA, Xu H, Clifton LA, Hughes A V., Webster JRP, et al. (2017)
522 Implications of lipid monolayer charge characteristics on their selective interactions
523 with a short antimicrobial peptide. *Colloids Surfaces B Biointerfaces* [Internet]. **150**,
524 308–316. Available from: <http://dx.doi.org/10.1016/j.colsurfb.2016.10.043>
- 525 [61] Gong H, Hu X, Liao M, Fa K, Ciumac D, Clifton LA, et al. (2021) Structural
526 Disruptions of the Outer Membranes of Gram-Negative Bacteria by Rationally
527 Designed Amphiphilic Antimicrobial Peptides. *ACS Appl. Mater. Interfaces* [Internet].
528 **13**, 16062–16074. Available from: <https://pubs.acs.org/doi/10.1021/acsami.1c01643>
- 529 [62] Nielsen JE, Lind TK, Lone A, Gerelli Y, Hansen PR, Jenssen H, et al. (2019) A
530 biophysical study of the interactions between the antimicrobial peptide indolicidin and
531 lipid model systems. *Biochim. Biophys. Acta - Biomembr.* [Internet]. **1861**, 1355–
532 1364. Available from:
533 <https://linkinghub.elsevier.com/retrieve/pii/S0005273619300823>
- 534 [63] Paracini N, Clifton LA, Skoda MWA, Lakey JH. (2018) Liquid crystalline bacterial
535 outer membranes are critical for antibiotic susceptibility. *Proc. Natl. Acad. Sci.*
536 [Internet]. , 201803975. Available from:
537 <http://www.pnas.org/lookup/doi/10.1073/pnas.1803975115>
- 538 [64] Le Brun AP, Zhu S, Sani M-A, Separovic F. (2020) The Location of the Antimicrobial
539 Peptide Maculatin 1.1 in Model Bacterial Membranes. *Front. Chem.* [Internet]. **8**.
540 Available from: <https://www.frontiersin.org/article/10.3389/fchem.2020.00572/full>
- 541 [65] Hoogerheide DP, Noskov SY, Jacobs D, Bergdoll L, Silin V, Worcester DL, et al.
542 (2017) Structural features and lipid binding domain of tubulin on biomimetic

- 543 mitochondrial membranes. Proc. Natl. Acad. Sci. [Internet]. **114**, E3622–E3631.
544 Available from: <http://www.pnas.org/lookup/doi/10.1073/pnas.1619806114>
- 545 [66] Soubias O, Pant S, Heinrich F, Zhang Y, Roy NS, Li J, et al. (2020) Membrane surface
546 recognition by the ASAP1 PH domain and consequences for interactions with the
547 small GTPase Arf1. Sci. Adv. [Internet]. **6**, eabd1882. Available from:
548 <https://advances.sciencemag.org/lookup/doi/10.1126/sciadv.abd1882>
- 549 [67] Holt SA, Le Brun AP, Majkrzak CF, McGillivray DJ, Heinrich F, Lösche M, et al.
550 (2009) An ion-channel-containing model membrane: structural determination by
551 magnetic contrast neutron reflectometry. Soft Matter [Internet]. Available from:
552 <http://xlink.rsc.org/?DOI=b822411k>
- 553 [68] Isaksson S, Watkins EB, Browning KL, Kjellerup Lind T, Cárdenas M, Hedfalk K, et
554 al. (2017) Protein-Containing Lipid Bilayers Intercalated with Size-Matched
555 Mesoporous Silica Thin Films. Nano Lett. [Internet]. **17**, 476–485. Available from:
556 <https://pubs.acs.org/doi/10.1021/acs.nanolett.6b04493>
- 557 [69] Shen HH, Leyton DL, Shiota T, Belousoff MJ, Noinaj N, Lu J, et al. (2014)
558 Reconstitution of a nanomachine driving the assembly of proteins into bacterial outer
559 membranes. Nat. Commun. [Internet]. **5**, 1–10. Available from:
560 <http://dx.doi.org/10.1038/ncomms6078>
- 561 [70] Hughes GW, Hall SCL, Laxton CS, Sridhar P, Mahadi AH, Hatton C, et al. (2019)
562 Evidence for phospholipid export from the bacterial inner membrane by the Mla ABC
563 transport system. Nat. Microbiol. [Internet]. Available from:
564 <http://dx.doi.org/10.1038/s41564-019-0481-y>
- 565 [71] McGillivray DJ, Valincius G, Heinrich F, Robertson JWF, Vanderah DJ, Febo-Ayala
566 W, et al. (2009) Structure of Functional Staphylococcus aureus α -Hemolysin Channels
567 in Tethered Bilayer Lipid Membranes. Biophys. J. [Internet]. **96**, 1547–1553.
568 Available from: <http://www.sciencedirect.com/science/article/pii/S0006349508032311>
- 569 [72] Gerelli Y. (2020) Applications of neutron reflectometry in biology. EPJ Web Conf.
570 [Internet]. **236**, 04002. Available from: [https://www.epj-](https://www.epj-conferences.org/10.1051/epjconf/202023604002)
571 [conferences.org/10.1051/epjconf/202023604002](https://www.epj-conferences.org/10.1051/epjconf/202023604002)
- 572 [73] Wacklin HP. (2010) Neutron reflection from supported lipid membranes. Curr. Opin.

- 573 Colloid Interface Sci. [Internet]. **15**, 445–454. Available from:
574 <http://dx.doi.org/10.1016/j.cocis.2010.05.008>
- 575 [74] Lakey JH. (2019) Recent advances in neutron reflectivity studies of biological
576 membranes. *Curr. Opin. Colloid Interface Sci.* [Internet]. **42**, 33–40. Available from:
577 <https://linkinghub.elsevier.com/retrieve/pii/S135902941930007X>
- 578 [75] Heinrich F, Lösche M. (2014) Zooming in on disordered systems: neutron reflection
579 studies of proteins associated with fluid membranes. *Biochim. Biophys. Acta*
580 [Internet]. **1838**, 2341–9. Available from:
581 <http://www.ncbi.nlm.nih.gov/pubmed/24674984>
- 582 [76] Fragneto G, Delhom R, Joly L, Scoppola E. (2018) Neutrons and model membranes:
583 Moving towards complexity. *Curr. Opin. Colloid Interface Sci.* [Internet]. **38**, 108–
584 121. Available from: <https://linkinghub.elsevier.com/retrieve/pii/S135902941830030X>
- 585 [77] Clifton LA, Hall SCL, Mahmoudi N, Knowles TJ, Heinrich F, Lakey JH. (2019)
586 Structural Investigations of Protein–Lipid Complexes Using Neutron Scattering
587 [Internet]. In: Kleinschmidt JH, editor. *Lipid-protein interactions. Methods in*
588 *Molecular Biology*. New York, N.Y.: Humana Press; 2019. p. 201–251. Available
589 from: http://link.springer.com/10.1007/978-1-4939-9512-7_11
- 590